Integrated modeling of optical performance for the Terrestrial Planet Finder structurally connected interferometer

David M. LoBosco[a], Carl Blaurock[b], Soon-Jo Chung[a], and David W. Miller[a]

[a]Massachusetts Institute of Technology, 77 Massachusetts Ave, Cambridge, MA 02139, USA;
[b]Midé, 200 Boston Ave, Suite 1000, Medford, MA 02155 USA

ABSTRACT

The Terrestrial Planet Finder (TPF) mission, to be launched in 2014 as a part of NASA's Origins Program, will search for Earth-like planets orbiting other stars. One main concept under study is a structurally connected interferometer. Integrated modeling of all aspects of the flight system is necessary to ensure that the stringent dynamic stability requirements imposed by the mission are met.

The MIT Space Systems Laboratory has developed a suite of analysis tools known as DOCS (Disturbances Optics Controls Structures) that provides a MATLAB® environment for managing integrated models and performing analysis and design optimization. DOCS provides a framework for identifying critical subsystem design parameters and efficiently computing system performance as a function of subsystem design. Additionally, the gradients of the performance outputs with respect to design variables can be analytically computed and used for automated exploration and optimization of the design space.

The TPF integrated model consists of a structural finite element model, optical performance model, reaction wheel isolation stage, and attitude/optical control systems. The integrated model is expandable and upgradeable due to the modularity of the state-space subsystem models. Optical performance under reaction wheel disturbances is computed, and the effects of changing design parameters are explored. The results identify redesign options that meet performance requirements with improved margins, reduced cost and minimized risk.

Keywords: Integrated modeling, TPF, structural dynamics, controls, optical performance, disturbances, interferometer, structurally connected

1. INTRODUCTION

NASA will launch the Terrestrial Planet Finder (TPF) in 2014 to search for Earth-like planets orbiting other stars. This flagship of the Origins Program is still in its early design phase and many architecture trades are being performed. One architecture currently being studied is a large baseline nulling interferometer. The interferometer will consist of four, 3-4 m diameter telescopes structurally connected or formation flown along a 40 m or greater baseline operating at cryogenic temperatures of approximately 40 Kelvin and collecting light in the infrared spectrum. Nulling interferometry uses destructive and constructive interference of multiple separated telescopes to block the star light and amplify the reflected light from the orbiting planet.[1]

In order to determine if this, or any, architecture will achieve the the stringent optical performance requirements for TPF, integrated modeling is necessary. The structural dynamics, controls, optics and disturbances sources must all be modeled so that their combined effects on optical performance are understood.

In this paper we will develop an integrated model of the structurally connected interferometer (SCI) for TPF. Its purpose will be to predict optical performance and be used in design trades to determine ways to improve optical performance. Given that TPF is still in its early development phase, it is expected that many parameters will change throughout the design process. Therefore, it is important that the integrated model is easily adaptable and evolvable as the design progresses and the requirements are better understood.

Further author information: E-mail: lobosco@mit.edu, Telephone: (617) 258-6872

Modeling and Systems Engineering for Astronomy, edited by Simon C. Craig, Martin J. Cullum, Proc. of SPIE Vol. 5497 (SPIE, Bellingham, WA, 2004)
0277-786X/04/$15 doi: 10.1117/12.550929

To generate our integrated model we will use the DOCS (Disturbances-Optics-Controls-Structures) toolbox created by the MIT Space Systems Laboratory and Midé Technology Corporation. DOCS provides a powerful framework for the modeling and analysis of precision opto-mechanical space systems. Utilizing the MATLAB environment, DOCS allows the user to create an integrated model of the spacecraft that simulates the structural dynamics, controllers, and optical layout. DOCS elements are created as state space objects and integrated models are generated by linking DOCS elements together. By creating the integrated models in state-space form it is easy to upgrade existing subsystem models or add new subsystem models while keeping inputs and outputs consistent. The integrated models can be converted to the frequency domain to utilize stochastic broadband disturbance models. Disturbances are input into the system and root mean square optical performance metrics are calculated as the outputs.

Using the DOCS toolbox, we can also analyze the integrated model in many ways. First, we can vary certain design parameters without re-running the entire model and determine the effect on performance. This allows us to determine the sensitivity of performance to each design parameter and figure out which aspects of the design have the most effect on the overall performance. Moreover, we can produce modal variance contribution plots that allow for the identification of problematic vibration modes in the structure. Recommendations can then be made to either redesign part of the structure or prevent disturbances in the problematic frequency ranges.

1.1. Integrated Model Overview

The entire integrated model generation and optical performance analysis is automated through the use of MATLAB. The user provides design variable inputs to a MATLAB function and optical performance outputs are returned. The inputs define geometry, material properties, control bandwidths, etc. for the different subsystem models. The integrated model can adapt to changes in these design variables and be automatically regenerated.

Figure 1 shows a block diagram of the integrated model of TPF. The plant consists of the dynamics of the spacecraft structure derived from a finite element model. The main disturbance input to the plant comes from the reaction wheel imbalances. A stochastic broadband reaction wheel disturbance model passes through a low-pass filter isolator before entering the plant. A linear optical sensitivity matrix is generated using the CODE-V® optical modeling software. The sensitivity matrix relates the motion of critical nodes in the finite element model to the desired optical performance metrics. Optical sensor noise is added to the performance outputs before they enter the optical controllers (modeled as high-pass filters). The output of the optical controllers is optical performance.

2. INTEGRATED MODELING THEORY

In this section we will develop the theory behind our integrated modeling and performance analysis methods.

2.1. Structural Dynamics Model

The structural model begins in the time domain with physical coordinates in second order form. It is then transformed into modal coordinates so that modal damping may be added. The modal, time domain model is then converted into state-space, first order form so that it may be linked to other components of the integrated model.

2.1.1. Time Domain Model

The dynamics of a multi-degree-of-freedom system are described in the time domain by the equation

$$\mathbf{M}\ddot{\mathbf{x}} + \mathbf{K}\mathbf{x} = \mathbf{f} \tag{1}$$

where $\mathbf{M}$ is the mass matrix, $\mathbf{K}$ is the stiffness matrix, and $\mathbf{f}$ is a vector of forcing functions. The motion of each degree of freedom is described by the elements contained in the vector $\mathbf{x}$. In our model, the structure will be represented by a multi-degree-of-freedom finite element model (FEM). The FEM will be described in more detail in Section 3. The finite element analysis software, NASTRAN® in our case, uses the information in the bulk data deck to generate the mass and stiffness matrices. It then calculates a matrix of eigenvectors, Φ, and

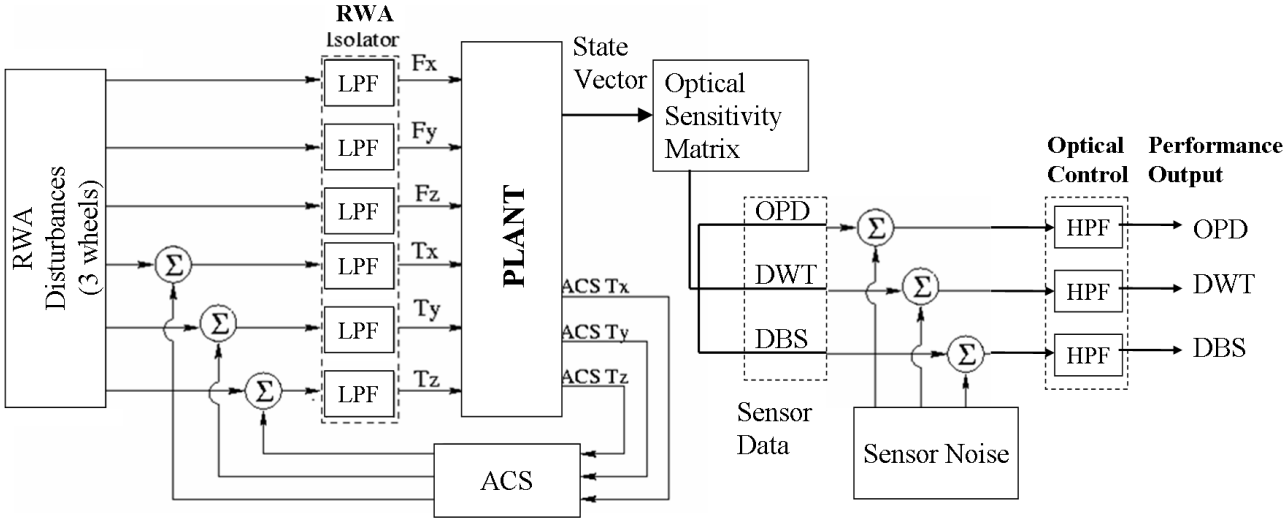

Figure 1. Block diagram of integrated model

a diagonal matrix of eigenvalues, λ. The eigenvectors in the matrix, Φ, define the mode shapes of the system. The elements of the diagonal eigenvalue matrix, λ, give the natural frequencies by the relation

$$\lambda_{i,i} = \omega_i^2 \tag{2}$$

where ω_i is the natural frequency of mode i.

Using the eigenvectors, we convert our equations of motion from physical coordinates, $\mathbf{x}$, to modal coordinates, $\mathbf{q}$, through the transformation

$$\mathbf{x} = \Phi\mathbf{q}. \tag{3}$$

Our eigenvalues are mass normalized so that $\Phi^T\mathbf{M}\Phi = I$. Using this and the relation, and recognizing that $\omega^2 = \mathbf{M}^{-1}\mathbf{K}$, our modal equations of motion are

$$\ddot{\mathbf{q}} + \omega^2\mathbf{q} = \Phi^T\mathbf{f}. \tag{4}$$

By representing the dynamics of the system in modal form in Equation 4, we have created a set of elastically and inertially uncoupled equations of motion. This is useful because it provides us an easy way to add damping. Whereas the stiffness matrix relates forces to displacements, damping is modeled as a nonconservative resistive force proportional to the velocity of each degree of freedom. In this case, the resistive forces are proportional to the velocity of the modal degrees of freedom, $\dot{\mathbf{q}}$. With the addition of modal damping, Equation 4 becomes

$$\ddot{\mathbf{q}} + 2\zeta\omega^2\dot{\mathbf{q}} + \omega^2\mathbf{q} = \Phi^T\mathbf{f} \tag{5}$$

where ζ is the modal damping ratio. In our model we will use a nominal value of $\zeta = 0.001$

2.1.2. State-Space Representation/Optical Model

The time domain model with modal coordinates is converted to state-space form for two main reasons. The first is for the ease of linking independent models in order to create a large integrated model of a complex system like TPF. The second is to utilize the output equation that relates the motion of physical points in the structure to the desired performance metrics. This output equation will be used to implement the optics model.

Our multi-degree-of-freedom system is represented in the state-space domain by converting Equation 5 into

$$\dot{\hat{q}} = A\hat{q} + Bu \tag{6}$$

with the output equation

$$y = C\hat{q}. \tag{7}$$

The state vector is

$$\hat{q} = \left\{ \begin{array}{c} \mathbf{q} \\ \dot{\mathbf{q}} \end{array} \right\}, \tag{8}$$

and the system matrix is

$$A = \left(\begin{array}{cc} 0 & I \\ -\omega^2 & -2\zeta\omega \end{array} \right). \tag{9}$$

The vector u is the forcing input term. It will apply the disturbance input, f, from Equation 5. The pointing vector is

$$B = \left(\begin{array}{c} 0 \\ \Phi^T \end{array} \right). \tag{10}$$

2.2. Disturbance Modeling/Performance Analysis

Recent work has shown that reaction wheel disturbances can be more easily modeled in the frequency domain as power spectral density (PSD) functions than in the time domain.[2,3] Therefore, in order to utilize this PSD disturbance source, we must move our state-space model into the frequency domain. First, we take the Laplace Transform of Equation 6:

$$\hat{Q}(s)s = A\hat{Q}(s) + BU(s). \tag{11}$$

Rearranging Equation 11 and substituting it into the Laplace Transform of Equation 7 we find that

$$Y(s) = C(sI - A)^{-1}BU(s). \tag{12}$$

Now, the transfer function of disturbance input to performance output is found:

$$G(s) = U(s)^{-1}Y(s) = C(sI - A)^{-1}B. \tag{13}$$

As shown in Brown and Hwang, the output PSD of a transfer function with PSD input $S_U(s)$ is

$$S_Y(s) = G(s)S_U(s)G^H(s) \tag{14}$$

where $G^H(s)$ is the "Hermetian", or complex conjugate transpose, of $G(s)$.[4] An effective way of measuring performance is to find the root-mean-square (RMS) of the output PSD. The mean-square value is first found by

$$\sigma_Y^2 = E(Y^2) = \frac{1}{2\pi j}\int_{-j\infty}^{j\infty} S_Y(s)ds. \tag{15}$$

This is the same as taking the variance of the output since ours is a zero-mean system.[5] The RMS is found by taking the square root of the mean-square value. We now have a complete method by which to analyze the performance of our multi-degree-of-freedom system.

3. FINITE ELEMENT MODEL

As described in Section 2.1, the FEM is used to create a multi-degree-of-freedom system that will represent the "plant." Our MATLAB code automatically generates the FEM bulk data deck, runs the finite element analysis and extracts the eigenvectors and eigenvalues to build the state-space structural dynamics model.

The FEM consists of a 40 m truss with four evenly spaced collectors. Nominally, the truss elements use aluminum material properties. The mirrors are given beryllium mass properties and an areal density of 15 kg/m^2 to meet the lightweight optics requirement of other advanced space-based telescopes.[6] The mirror modulus is given a stiffness 100 times that of beryllium to represent a stiffening honeycomb support structure. The mirror supports are also given a stiff modulus of 100 times that of aluminum to place the mirror tip/tilt vibration modes at a realistic frequency. Finally, the bus and optics combiner are represented as point masses at the center of the truss. The full finite element model of TPF SCI is shown in figure 2.

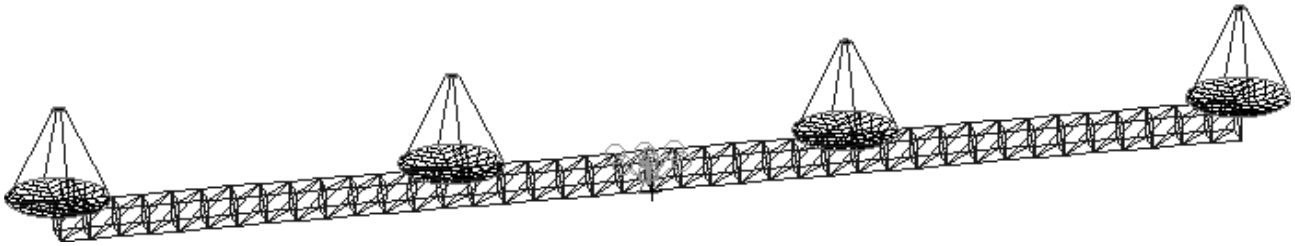

Figure 2. Full finite element model

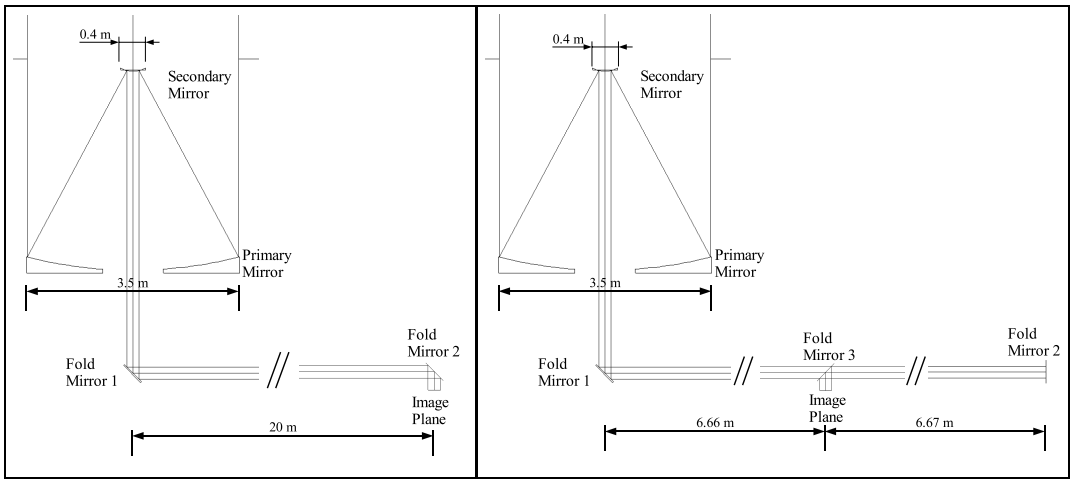

(a) (b)

Figure 3. Optical layout of (a) aperture one and (b) aperture two.

4. OPTICAL MODEL

In this section we will provide an overview of the optical layout, explain the optical performance metrics and derive the partial derivatives relating the motion of critical nodes in the FEM to these performance outputs. These partial derivatives are used to assemble the optical sensitivity matrix.

4.1. Optical Layout

The optical model is generated in CODE-V. The layout of each aperture consists of a primary mirror, secondary mirror, fold mirrors and an image plane. The optical prescription defining the primary mirrors for each aperture is identical and the optical prescription for each secondary mirror is identical. The fold mirrors are arranged in such a way to direct the light towards the center of the spacecraft and create equal pathlengths for each aperture.

Figure 3 shows ray traces for aperture one and aperture two. Due to the symmetry of the spacecraft, the layout of aperture three is a mirror image of that for aperture two. Likewise, the layout of aperture four is a mirror image of the layout for aperture one. These four optical models will be used to calculate the optical performance sensitivities.

4.2. Optical Performance Metrics

When modeling any spacecraft, relevant metrics must be assigned to accurately predict performance. These metrics are used to verify that mission requirements will be met, or to help in the redesign process if it is found that the mission requirements will not be met.

Table 1. Nominal performance requirements.

Performance Metric	Requirement
OPD	1.01 nm
DWT	50.81 nrad
DBS	1.59 μm

The main optical requirements for TPF are Null Depth and Null Stability.[7] A flow-down will be performed to determine the requirements on factors that contribute to Null Depth and Null Stability degradation. In this model, we will focus on the contributing factors of Optical Pathlength Difference (OPD), Differential Wavefront Tilt (DWT) and Differential Beam Shear (DBS). First, OPD is the difference in pathlength between two apertures. In order for interferometry to occur, all pathlengths must be equal to within a small fraction of the wavelength of light being observed. Secondly, the angles at which the light from different apertures hit the image plane must also be closely aligned. The measurement of error in this angular alignment is known as DWT. If there is significant DWT, the centerline may have zero OPD while OPD across the wavefront cross-section will grow as a function of distance from the center line. Lastly, DBS measures the error in overlap of beams from different apertures. Beams must overlap almost perfectly for optimal optical performance. If there is too much beam shear, not only will interferometry break down but the image that does come through will become blurry. The effect of disturbances on the spacecraft will be measured by OPD, DWT and DBS. Although exact requirements have not yet been set, we will use the values of "OPD jitter," "pointing jitter," and "beam walk modulation" from the example dual-Bracewell interferometer performance requirements flow-down from Noecker et. al. to set the requirements for OPD, DWT, and DBS in our analysis.[7] The values for these requirements are shown in Table 1.

4.3. Partial Derivative Methods

A linear optical model must be created to relate the motion of nodes in the finite element model to the performance outputs. The linear sensitivities (or partial derivatives) are obtained by using the three step process described by Howard.[8]

1. Perturb a single degree of freedom by a small representative value in the range expected due to the modeled disturbances.
2. Extract data from a ray trace to determine the optical performance metric.
3. Divide the performance metric by the magnitude of the perturbation to find the partial derivative.

This method is implemented through a set of MATLAB functions that interface with CODE-V. One MATLAB function computes the pathlength derivatives, the second finds the Wavefront tilt derivatives, and the last calculates the beam shear derivatives. Inputs to the MATLAB functions include the CODE-V file name, the number of mirrors, the coordinates of the ray to be traced, the magnitude of the linear and rotational perturbations, and the static tilt for each mirror.

4.4. The Optical Sensitivity Matrix

Each mirror from the optical model is mapped to its nearest critical node in the FEM. There is one critical node at the center of each primary and secondary mirror, plus one at the location of the combiner for a total nine critical nodes. These mapped sensitivities are used to generate a matrix that when multiplied by the state vector will produce the values of OPD, DWT_x, DWT_y, DBS_x, and DBS_y between apertures 1&2, 1&3, and 1&4. This is our optical sensitivity matrix.

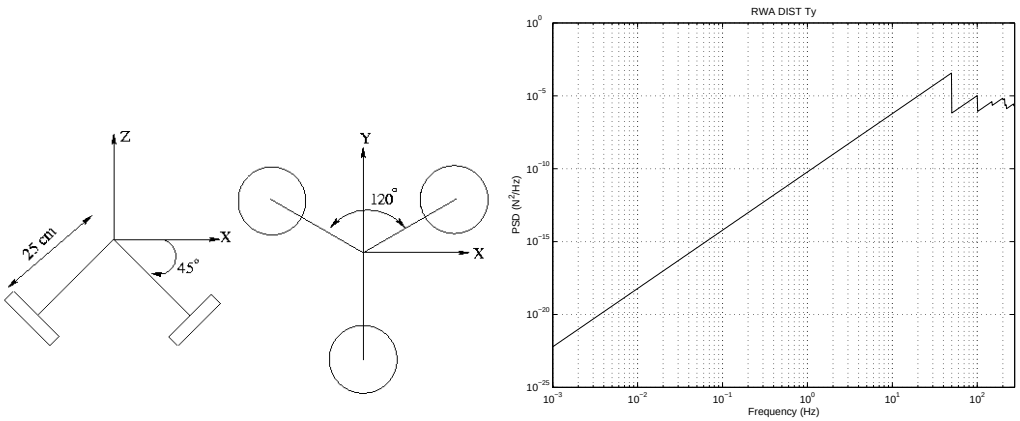

(a) (b)

Figure 4. (a)Reaction wheel assembly orientation. (b) Reaction wheel disturbance PSD (torque about y-axis).

5. DISTURBANCE MODEL

We choose to model two forms of disturbances in this analysis. First, we model static and dynamic imbalances in the reaction wheels since they are the largest disturbance source on most spacecraft. These disturbances are inputs to the plant and apply forces and torques about all six degrees of freedom. Secondly, we model sensor noise since it will likely be a driving factor in meeting the null stability requirement. This disturbance is added to the outputs of the optical sensitivity matrix and degrades the inputs to the optical controllers.

5.1. Reaction Wheel Disturbances

Reaction wheel imbalance is the largest source of disturbances for most spacecraft. As such, it is very important to understand the effects of these disturbances on spacecraft performance. Much work has been done on modeling reaction wheel disturbances in recent years. Melody developed a stochastic broadband modeling method for reaction wheel disturbances.[2] His work focused on the Hubble Space Telescope wheels but the method is applicable to all wheels. Masterson used Melody's method to develop models of the Ithaco B-type and Ithaco E-type wheels.[3]

For our analysis, we will use Masterson's power spectral density disturbance model of the Ithaco E-type wheel. The Ithaco wheel used to generate this model was an off-the shelf product that had not been balanced for "minimum vibration operation".[3] Three of these wheels are used and placed at the center of the spacecraft truss in an orientation explained in Figure 4(a). Using the experimental data of the Ithaco E-type wheel, disturbance PSDs are generated for all six degrees of freedom (3 forces and 3 moments). Figure 4(b) shows the disturbance spectrum for one of these degrees of freedom. Data is generated for wheels operating from 0-3000 RPM with a frequency range of 0-278 Hz.

5.2. Sensor Noise

In order to achieve optical requirements, a set of controllers will be used to minimize OPD, DWT, and DBS. This control capability will likely be implemented with fast steering mirrors (FSMs) and optical delay lines (ODLs). A suite of sensors will measure the optical error and provide inputs to the controller. However, perfect measurements cannot be made due to sensor noise. One example is fine guidance sensor error arising from photon noise.[9] Contributing factors to this error include detector quantum efficiency, integration time and guide star magnitude.[9] Precise sensor models for TPF, however, are not available at this time. Therefore, as a start, we model sensor noise as providing an RMS error equal to half the requirement for OPD, DWT, and DBS.

Sensor noise is modeled as a low-pass shaping filter with a white noise input. This is done so that a PSD can be generated and used in our frequency domain analysis. The transfer function of the low-pass filter, $G_{LP}(s)$, takes the form

$$G_{LP}(s) = \frac{bc}{s-a} \tag{16}$$

where bc is the gain, a is the cutoff frequency, and a, b, and c are 1×1 matrices in the state-space equations.

By driving this filter with a PSD input $S_{uu}(s)$, the output PSD is found by evaluating the expression

$$S_{xx}(s) = G_{LP}(s)S_{uu}(s)G_{LP}(s)^H \tag{17}$$

where $G_{LP}(s)^H$ is the complex conjugate transpose of $G_{LP}(s)$. For a unity white noise input, $S_{uu}(s) = 1$, Equation 17 reduces to

$$S_{xx}(s) = G_{LP}(s)G_{LP}(s)^H. \tag{18}$$

The mean square value of the output is given by

$$E[x^2] = \frac{1}{2\pi j}\int_{-j\infty}^{j\infty} S_{xx}(s)ds. \tag{19}$$

In G_{LP}, the values for a and b are set equal to the bandwidth of the optical controller, f_{oc}. We solve for c by setting $E[x^2]$ equal to the performance requirement and using and integral table from Brown & Hwang.[4]

6. DISTURBANCE REJECTION

As stated in the previous section, the primary source of disturbances for TPF will likely be caused by the imbalance of the rotating reaction wheels. If the vibrations from this disturbance are not properly attenuated, the optical performance requirements will never be met. One mitigation strategy is to use a combination of high frequency attenuation at the disturbance input and low frequency attenuation at the performance output.[10]

6.1. Reaction Wheel Vibration Isolation System

In practice, the job of high frequency disturbance attenuation will be done by a combination of passive and active vibration isolation. The idea is to allow the low frequency torques to be passed into the spacecraft bus to perform the attitude adjustments while blocking out the high frequency disturbances that will degrade optical performance. Typically a six-axis "hexapod" active reaction wheel assembly (RWA) vibration isolator will be used. Each strut of the hexapod contains a diaphragm, which acts as a soft spring, and a voice coil actuator. The diaphragm acts as the passive isolator while the voice coil performs active vibration isolation through feedback control.[10]

For early design trades such as our TPF analysis, we can model the RWA isolator as a second order low pass filter with transfer function

$$G_{iso} = \frac{(2\pi f_{iso})^2}{s^2 + 2\zeta_{iso}(2\pi f_{iso})s + (2\pi f_{iso})^2} \tag{20}$$

where f_{iso} is the cutoff frequency and ζ_{iso} is the damping ratio. The nominal values are $f_{iso} = 10$Hz and $\zeta_{iso} = 0.4$.

The proper relationship between RWA isolator cutoff frequency and optical control bandwidth must be found so that the two attenuation methods compliment one another while minimizing the disturbance leakage. We therefore set the cutoff frequency to be a DOCS perturbable design parameter so that optimizations may be performed later.

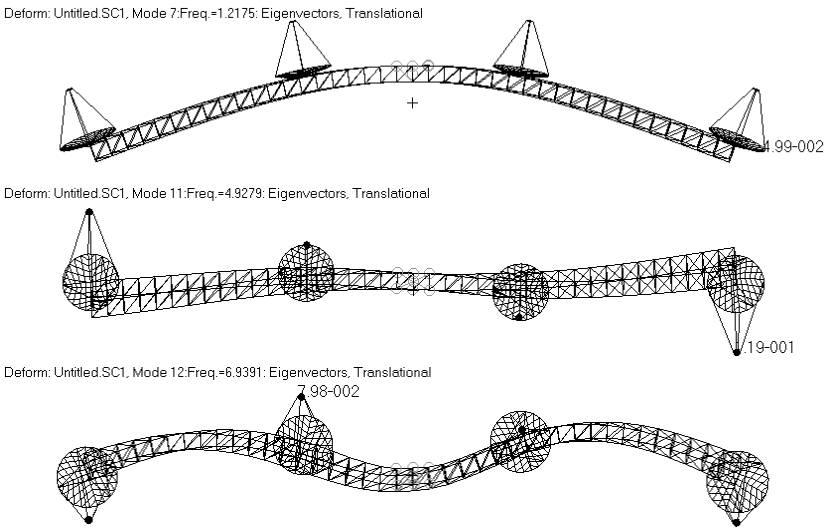

Figure 5. Selected mode shapes

6.2. Optical Control System

Low frequency attenuation is performed by active optical controllers located along the optical train. In practice, actuators such as fast steering mirrors (FSMs) and optical delay lines (ODLs) will be used for the optical control. FSMs can tip and tilt to alter the wavefront tilt of the incoming beam of light. An ODL uses piston movement to change the overall pathlength of the light beam.

In order to simplify our analysis, the effects of the optical controllers are modeled as first order high pass filters. The transfer function for the optical control filter is

$$G_{oc}(s) = \frac{s}{s + (2\pi f_{oc})} \tag{21}$$

where the nominal cutoff frequency, f_{oc}, is 100 Hz. We want the control bandwidth to be high enough to attenuate enough of the performance errors to meet the requirements. The main limiting factor on bandwidth is computational cost. Therefore, the control bandwidth is also set as a DOCS perturbable design parameter so that trade studies and design optimizations can be performed.

As described in section 5, sensor noise is added to the performance outputs of the integrated model before they are sent through the optical control filter. The final performance values for OPD, DWT and DBS come from the output of the optical controller.

6.3. Attitude Control System

An attitude control system (ACS) will provide the pointing stability for TPF. Rotational rigid body modes are contained in the structural model that, without the use of an ACS, will hinder the optical performance. The ACS is modeled as a proportional-derivative controller using a predefined DOCS function. The control bandwidth is set to 0.01 times the first mode frequency of the plant. This is done to prevent interaction between the controller and the flexible modes of the structure. The bandwidth can be altered by changing the appropriate design variable input.

7. OPTICAL PERFORMANCE ANALYSIS

In this section we link together the different individual models to create the full integrated model. The disturbance analysis is then performed and RMS optical performance outputs are calculated. Using the DOCS toolbox, we make certain design parameters perturbable. This allows us to determine how to improve performance without having to regenerate the FEM over and over again.

Table 2. First six non-rigid body modes

Mode No.	Frequency (Hz)	Description
7	1.22	1st bending about y-axis
8	1.25	1st bending about z-axis
9	3.92	2nd bending about z-axis
10	3.97	2nd bending about y-axis
11	4.93	Torsion mode. Apertures 1&2 in phase, 3&4 in phase
12	6.94	Torsion mode. Apertures 1&4 in phase, 2&3 in phase

Table 3. TPF mass breakdown.

Component	Mass (kg)
Truss	585
Bus	520
Combiner	430
RWA	32
Collectors	639
Total	**2206**

7.1. Nominal Performance

First, we will look at the nominal performance of the integrated model. The three main performance metrics are Optical Pathlength Difference (OPD), Differential Wavefront Tilt (DWT) and Differential Beam Shear (DBS). In addition to these performance metrics, we extract spacecraft mass, mode shapes and frequencies. These are also important characteristics to keep in mind when designing a spacecraft.

The first six modes of the FEM are all rigid body modes with frequencies nearly equal to zero. Table 2 lists the first six flexible modes (modes 7-12) along with the corresponding frequencies and a description of the mode shapes. Selected mode shapes, generated by the PATRAN® post-processor, are shown in Figure 5. The spacecraft mass breakdown is listed in Table 3.

Different components of the integrated model can be used as desired. For example, one may want to create an integrated model with and without the RWA isolator to observe its effect on performance. Four integrated model combinations are listed in Table 4 along with three of the nominal RMS performance outputs for each. We can see that the addition of optical control and RWA isolators dramatically improves the optical performance.

Figure 6(a) shows the transfer function of OPD13 over RWA disturbance torque about the y-axis. In the low frequency range we see that the ACS attenuates the rigid body mode. The bandwidth, located at the knee in the curve, is just above 0.01 Hz. This makes sense because our first flexible mode is just above 1 Hz. In Section 6 we set the ACS bandwidth to 0.01 times the first flexible mode frequency so that it does not interact with the dynamics of the structure.

Cumulative variance plots, like the one in Figure 6(b), essentially give us a running total of the integral that calculates mean square value. This allows us to see which modes in the system cause the most performance degradation. By examining this plot we see that there is a large jump in variance at a mode around 20 Hz. Once modes like this are identified, we can determine if strategies should be employed to prevent disturbances in the problematic region. For example, designers might decide that reaction wheels should not spin in certain speed ranges while optical observations are taking place. We can also look at the critical mode shape with a post-processor to determine if a specific area of the structure should be redesigned.

7.1.1. DOCS Perturbations

As seen in Table 4, our full integrated model comes close but does not meet the performance requirements. Redesign will be necessary if TPF is to achieve its observational goals. In this section we will use the DOCS system to perform design trades with the perturbable parameters designated during the integrated model generation.

During the integrated model generation we set RWA isolator cutoff frequency and optical control bandwidth to be DOCS perturbable parameters. Recall that the RWA isolators are modeled as second order low pass filters

Table 4. Nominal RMS values of OPD, DWT and DBS for each integrated model

Model Name	OPD12 (nm)	DWTx12 (nrad)	DBSx12 (μm)
Open loop	62.14	1090	62.47
Optical Control	12.31	204	17.26
RWA Isolator	53.08	909	14.01
RWA Iso. & Opt. Control	4.29	97	2.87

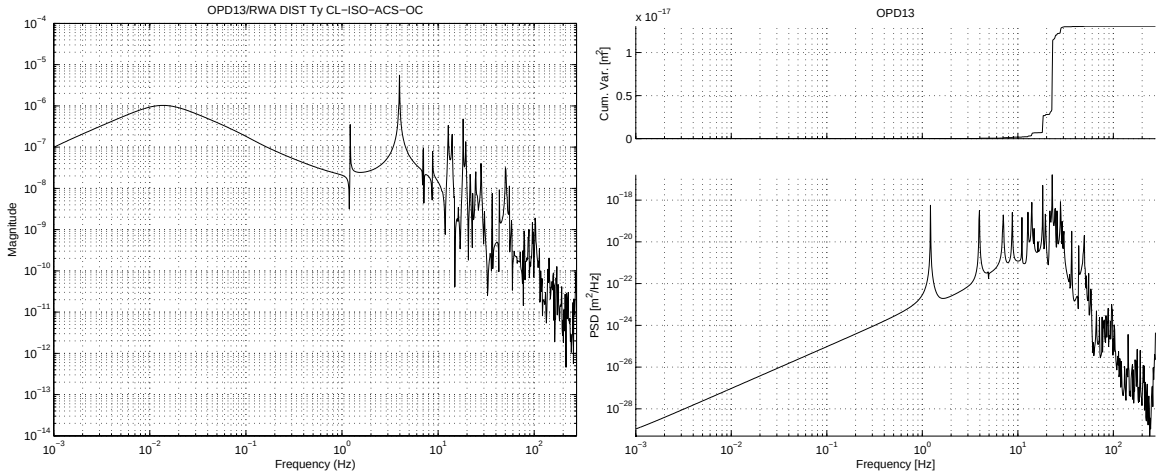

(a) (b)

Figure 6. (a) Transfer function of OPD13 over RWA disturbance Ty. (b) Cumulative variance PSD plot of OPD13

and the optical controllers are modeled as first order high pass filters. Each parameter can be varied individually to ascertain its effect on optical performance. It is more interesting, however, to vary both parameters in a nested loop to determine combined performance enhancement strategies.

Figure 7 shows two examples of isoperformance contour plots generated from varying both RWA isolator cutoff frequency and optical control bandwidth in a nested loop. By isoperformance we mean that there exists a range of design parameter combinations that will result in the same performance output. Any point on a curve marked with the same number will result in the same performance value. The OPD performance requirement of 1.01 nm is labelled as its own curve on the left-hand plot and the DWT requirement of 50.81 is labelled on the right-hand plot. Any point on or above these lines will define a combination of optical control bandwidth and RWA isolator cutoff frequency that will fall within requirements. We can also see from these curves that in general we want to decrease RWA isolator cutoff frequency and increase optical control bandwidth to improve performance. This trend is found across all of the performance metrics.

We must keep in mind the constraining trade offs not shown in Figure 7. As described in Section 6, the RWA isolator can be thought of as a spring-damper system. When cutoff frequency is reduced, this spring will get softer. As cutoff frequency approaches zero, the spring will effectively disappear and none of the torques for attitude control will be transferred to the structure. Therefore, one must set a minimum cutoff frequency based on the required low-frequency control authority. Likewise, optical control bandwidth has its own constraints such as computation costs and sensor limitations.

8. CONCLUSIONS

In this paper we have created an integrated model of the Structurally Connected Interferometer for TPF that can predict optical performance and be used in design trades. By creating the model in a modular state-space

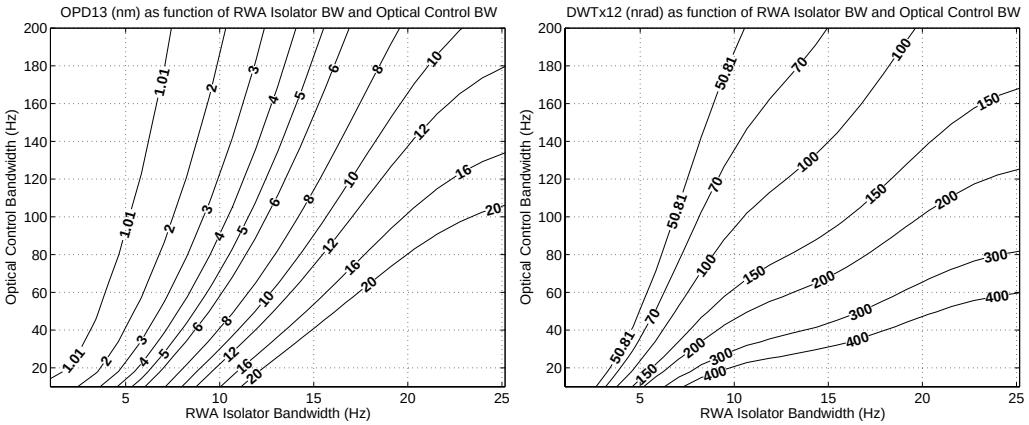

Figure 7. Isoperformance contours for OPD13 (left) and DWTx12 (right).

form using the DOCS environment, it is very upgradeable and expandable. Higher fidelity subsystem models can replace current models and new components can be added to the integrated model as the design process moves forward. Additionally, the integrated model generation is automated through the use of MATLAB allowing for easy regeneration with changes in a wide variety of design parameters.

ACKNOWLEDGMENTS

This research was performed for the Jet Propulsion Laboratory under JPL Contract #1250253 (TPF Interferometer Trades and Model Development) with Technical/Scientific Officers Dr. Curt Henry and Dr. Brent Ware, and JPL Contract #1255406 (Model Verification) with Technical/Scientific Officer Dr. Marie Levine-West. Ms. SharonLeah Brown served as MIT Fiscal Officer for both contracts.

REFERENCES

1. Alan Dressler, et. al., *Origins: Roadmap for the Office of Space Science Origins Theme*, Jet Propulsion Laboratory, 2003.
2. J. W. Melody, "Discrete-Frequency and Broadband Reaction Wheel Disturbance Models." JPL Interoffice Memorandum. June 1, 1995.
3. R. A. Masterson, "*Development and Validation of Empirical and Analytical Reaction Wheel Disturbance Models*," Master's thesis, Massachusetts Institute of Technology, June 1999.
4. R. Brown and P. Hwang, *Introduction to Random Signals and Applied Kalman Filtering*, John Wiley & Sons, 1997.
5. P. Wirsching, T. Paez, and K. Ortiz, *Random Vibrations*, John Wiley & Sons, 1995.
6. http://www.jwst.nasa.gov/.
7. C. Noecker, O. Lay, B. Ware, and S. Dubovitsky, "TPF interferometer performance requirements," *Proceedings of SPIE Vol. 5170 Techniques and Instrumentation for Detection of Exoplanets* , 2003.
8. J. M. Howard, "Optical Modeling Activities for the James Webb Space Telescope (JWST) Project: 1. The Linear Optical Model," *Optical Modeling and Performance Predictions, Proceedings of SPIE* **5178**, pp. 82–88, 2004.
9. O. de Weck, "*Integrated Modeling and Dynamics Simulation for the Next Generation Space Telescope*," Master's thesis, Massachusetts Institute of Technology, 1999.
10. G. W. Neat, J. W. Melody, and B. J. Lurie, "Vibration Attenuation Approach for Spaceborne Optical Interferometers," *IEEE Transactions on Control Systems Technology* **6**, pp. 689–700, November 1998.